Internal Rotation of Amino and Nitro Groups in TATB: MP2 Versus DFT (B3LYP)

M. Riad Manaa,* Richard H. Gee, and Laurence E. Fried

University of California, Lawrence Livermore National Laboratory, Chemistry and Materials Science Directorate, P.O. Box 808, L-282, Livermore, California 94551

Received: April 23, 2002; In Final Form: July 23, 2002

We report second-order Møller−Plesset (MP2) and density functional (B3LYP) fully optimized amino and nitro group torsional potential barriers in 1,3,5-triamino-2,4,6-trinitrobenzene (TATB), a molecule with unusually strong intramolecular hydrogen bonding. The calculated barriers show optimum values of 17.0 (25.5) kcal/mol for the amino group and 5.6 (10.5) kcal/mol for the nitro group rotation at the MP2 (B3LYP) level. The large barrier associated with the amino rotation is due to the double-bond character of the respective C−N bond. Because the B3LYP results are 50−87% higher in energy than those provided by MP2, a more detailed comparison with other functionals and higher-level ab initio methods is needed for an accurate description of these intramolecular motions.

I. Introduction

In the case of TATB (1,3, 5-triamino-2,4,6-trinitrobenzene, Figure 1), it is thought that strong intramolecular interactions are the major contributors to the extraordinarily low sensitivity to shock or impact of this explosive.[1] TATB's crystal structure consists of hydrogen-bonded molecular sheets, similar to graphite.[2] The intermolecular hydrogen bonding in this molecular solid also plays a role in its overall stability. These strong interactions are manifested by the lack of a distinct melting point, believed to be >300 °C, and by the total insolubility of this compound in most common solvents.[1,3] Reliable determinations of energy barrier and associated torsional potentials of the substituent groups (amino and nitro) are important quantifying measures of the strength of intramolecular interactions and for the development of potential energy functions for this system. The propensity toward such molecular deformations might help explain some peculiar physical properties of TATB. These include the observed permanent volume increase of powder composites between 214 and 377 K,[3] the thermally activated structure changes,[4] and the discovery of second harmonic generation (SHG) efficiency.[5,6]

In a recent article,[7] we reported the rotational barrier of the nitro group in TATB using second-order Møller−Plesset (MP2)[8] to be 11.0 kcal/mol and with density functional theory[9] using the hybrid gradient-corrected correlation functional B3LYP[10,11] to be 17.9 kcal/mol, employing the standard 6-311G** basis set. Even with the lower of the two results, the barrier is more than twice that of nitrobenzene and nitroethylene.[12,13] The relatively large barrier was attributed to the very strong intramolecular hydrogen bonding in this molecule, where the neighboring oxygen−hydrogen bond is 1.7−1.8 Å at the equilibrium structure and is well below the van der Waals limit of 2.62 Å.[14] Furthermore, the fully optimized torsional barrier was also determined at the B3LYP level, revealing the effect of nuclear relaxation with a maximum barrier of 10.5 kcal/mol. MP2 single-point calculations of the DFT optimized curve, however, lowered the barrier to 5.5 kcal/mol.

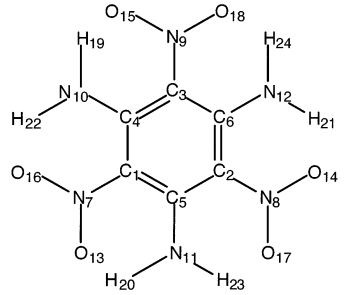

Figure 1. Molecular structure of TATB as referred to throughout the text.

The discrepancy between the MP2 and B3LYP results is significant enough that a comparative evaluation on equal footing is warranted. Because of their cost-effective nature, DFT methods have become widely used for studying the physical and chemical properties of relatively large molecules. The performance of DFT methods was shown early on to be generally no better than that of conventional ab initio techniques for geometries, dipole moments, and vibrational frequencies.[15] Recently, it was reported that the B3LYP calculated interaction energies for hydrogen-bonding systems were underestimated by up to 34% when compared with the CCSD(T) calculated limit[16] and that the PW91 functional[17] is a better alternative to ab initio methods. The deficiency in the B3LYP functional to evaluate the attraction between weakly bound systems properly was attributed to its erroneous asymptotic behavior at low density.[18,19] The recent study on the water dimer, however, an electrostatic or hydrogen-bonding-dominated system, reported the binding energy to be independent of both the basis set and the level of theory.[20] It is well-known that DFT-based methods do not include dispersion contributions that account for these types of interactions.[9] Because the development of a force field based on B3LYP calculations for large, energetic molecular systems such as HMX has recently been reported,[21] a similar attempt for TATB is currently underway in our group in order to model the thermally activated structural changes in this system properly. It is imperative, however, to scrutinize the accuracy of the B3LYP functional versus traditional (say MP2) ab initio

* Corresponding author. E-mail: manaa1@llnl.gov.

10.1021/jp0259972 CCC: $22.00
Published on Web 08/15/2002

TABLE 1: TATB Equilibrium Structure Molecular Parameters[a]

parameter	MP2	B3LYP	experiment[b]
	Bond Lengths		
R(C−C)	1.428	1.445	1.442
R(C−N) (amino)	1.343	1.326	1.314
R(C−N) (nitro)	1.445	1.440	1.419
R(N−O)	1.240	1.242	1.243
R(N−H)	1.009	1.014	
R(O−H)	1.802	1.702	
	Angles		
$C_1-C_4-C_3$	117.8	118.8	
$C_5-C_1-C_4$	122.1	121.1	
O−N−O	121.3	118.8	
C−N−O	119.2	120.6	
C−N−H	117.0	117.2	
H−N−H	123.1	125.5	
C−C−N (nitro)	119.1	119.4	
C−C−N (amino)	117.0	120.6	
	Dihedrals		
$C_3-C_4-C_1-C_5$	4.6	3.1	
N−C−C−N	6.9	4.2	
$O_{16}-N-C_1-C_4$	29.1	9.2	
$O_{13}-N-C_1-C_5$	22.6	4.1	
$O_{17}-N-C_2-C_5$	29.1	2.0	
$O_{14}-N-C_2-C_6$	22.6	3.6	
$O_{18}-N-C_3-C_6$	22.6	0.9	
$O_{15}-N-C_3-C_4$	29.1	3.8	
$H_{22}-N-C_4-C_1$	0.2	0.3	
$H_{19}-N-C_4-C_3$	21.5	4.7	
$H_{20}-N-C_5-C_1$	21.5	4.1	
$H_{23}-N-C_5-C_2$	0.3	1.3	
$H_{21}-N-C_6-C_2$	21.5	2.1	
$H_{24}-N-C_6-C_3$	0.2	2.5	

[a] Bonds in Å and angles in degrees. [b] From ref 2.

methods for internal rotations that involve strong interactions of neighboring groups.

In this work, we report the fully optimized amino ($-NH_2$) group torsional potential of TATB on the basis of the MP2 and B3LYP levels of treatment. We also report the MP2 fully optimized nitro ($-NO_2$) group torsional potential and compare it with our earlier DFT(B3LYP) calculation. The computational methods are used in conjunction with the 6-311G** basis set as implemented in the Gaussian 98 package of codes.[22] The choice of this basis set was shown to provide energies within 1.5 kcal/mol when compared with calculations employing the 6-311G++(2d, 2p) basis.[7] The reported calculations clearly reveal that the B3LYP method consistently produces results 40−85% higher than those determined with MP2 for these internal motions. Thus, the results should serve as a cautionary signal and should emphasize the need for further assessments with other high-level methods for systems with strong intramolecular hydrogen bonding.

II. Results and Discussion

A. Equilibrium Structure of TATB. X-ray analysis of the crystal structure of TATB[2] determined graphitelike sheet structure with two nearly planar molecules in a unit cell. No experimental information on the gas-phase structure has been reported. In Table 1, we list the molecular parameters of the equilibrium structure that was optimized without any symmetry constraints. As we noted previously[7] and reported in the Table, both B3LYP and MP2 bond distances compare reasonably well with those reported experimentally for the solid material.[2] Two important results are apparent, particularly for our later discussion of the energetics of rotational barriers.

First, the nearest-neighbor oxygen−hydrogen bond lengths, R(O−H), determined at the MP2 and B3LYP levels are 1.80 and 1.70 Å, respectively, which are significantly shorter than the van der Waals limit of 2.62 Å.[14] The discrepancy between these two results is due to the fact that the MP2-optimized structure is nonplanar and the nitro group is rotated with respect to the ring, thus increasing the O−H bond distance. Nevertheless, this is indicative of unusually strong intramolecular hydrogen bonding. The rotation of the respective functional groups will cause an increase in this bond length and will be a dominant factor in determining the associated barrier.

Second, the magnitude of the carbon−nitrogen bond of the amino group is shorter than that usually determined for a single bond. In Table 1, this bond is calculated to be 1.343 (1.326) Å at the MP2 (B3LYP) levels and is compared to the experimental value of 1.314 Å.[2] A typical value for a C−N single bond, however, is ∼1.45 Å, and that for a C−N double bond is 1.27 Å.[23] For TATB, then, the $C-NH_2$ bond certainly exhibits an admixture of double-bond character, which is not altogether unexpected when the conjugative interaction of the type shown in structure I below plays a role. The consequence of the presence of π character is to present much more resistance for the rotation around this bond, as discussed later.

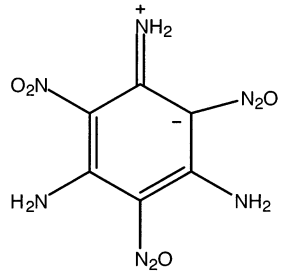

I

This characteristic is also demonstrated in the $C-NH_2$ bond energy, calculated to be 104.4 kcal/mol[7] at the B3LYP/6-311G** and 103.4 kcal/mol[24] at the BPW91/cc-PVDZ levels of theory.

The optimized bond angles are listed in Table 1, with the indices referring to the corresponding structure in Figure 1. The two methods produced bond angles with only 1−3° difference. As for the dihedrals, the most pronounced fact is the relatively large rotation of both the nitro and amino groups at the MP2 level, predicting ∠ONCC = 22−29° and ∠HNCC = 21.5° compared to recent calculations that showed ∠ONCC = 28° and ∠HNCC = 9° at the Hartree−Fock (HF) level using 6-31G*,[25] 6-311G**,[7] and cc-PVDZ[24] basis sets. The B3LYP results, however, yielded a nearly planar structure that is similar to the experimentally determined solid-phase structure. Earlier DFT calculations also determined a near-planar equilibrium molecular structure for ∠ONCC = 6.1 and −1.5° and ∠HNCC = −2.9 and −1.1° at the local-density approximation (LDA)/6-31G*[25] and BPW91/cc-PVDZ[24] levels, respectively.

That the B3LYP equilibrium structure is more closely related to the experimental structure of the crystal solid is by no means a testament to the accuracy of this method. The graphitelike sheets of TATB molecules in the crystals are stabilized by strong intermolecular hydrogen bonding that is completely neglected in locating the minimum-energy structure of an isolated TATB molecule. In the absence of gas-phase structural data, it is certainly possible that the true equilibrium structure is the nonplanar MP2-determined structure, which conforms to planarity only as those long-range interactions are accounted for in

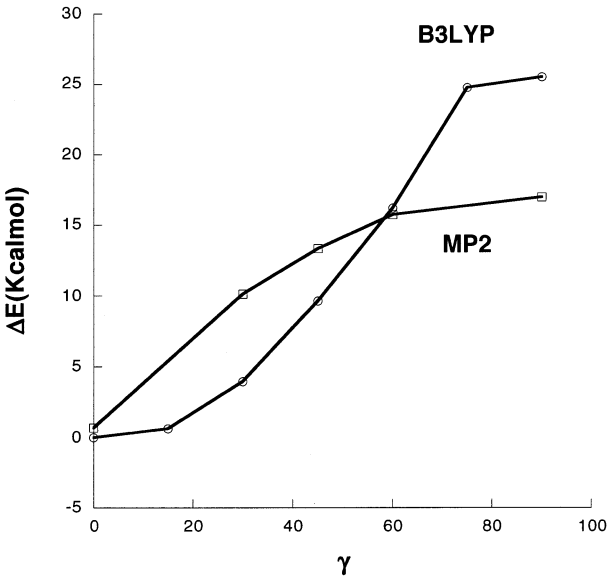

Figure 2. B3LYP and MP2 fully optimized $-NH_2$ torsional potentials.

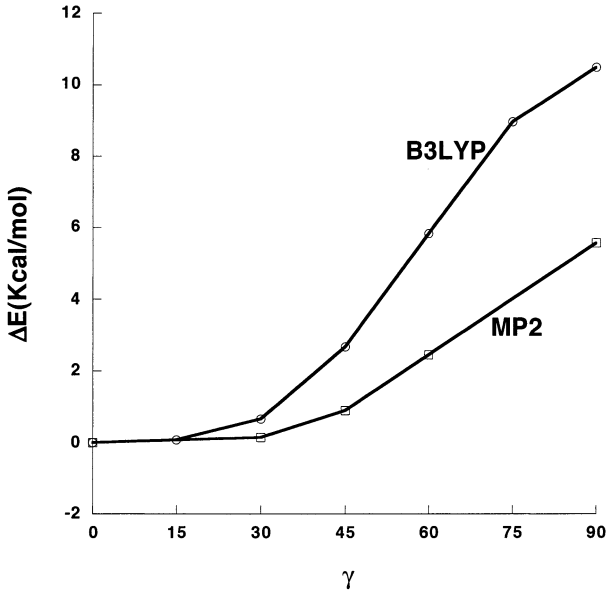

Figure 3. B3LYP and MP2 fully optimized $-NO_2$ torsional potentials.

the condensed phase. Energetically, this seems to be very plausible: an MP2 single-point calculation on the B3LYP planar structure is only 2.0 kcal/mol higher than the optimized MP2 equilibrium structure. Moreover, the MP2 minimum-energy pathway for the dihedral angles associated with the nitro group is nearly constant in the range of 0−30°, as discussed later (see Figure 3). This is consistent with the thermal motion analysis of the X-ray structure that predicted nitro group libration with an average torsional amplitude of 12°.[2] These observations lead to the conclusion that, although the MP2 minimum-energy structure exhibits partial rotations of the functional groups, the potential energy profile in the vicinity of this nuclear configuration and connecting to the planar condensed-phase structure is nearly flat.

B. Amino and Nitro Rigid-Body Rotational Barriers. The calculated amino and nitro rotational barriers, using a perpendicular conformation of these functional groups to that of the equilibrium structure, are presented in Table 2. Within this rigid-body treatment, these barriers represent upper bounds to the true rotational barriers in the gas phase, neglecting relaxation

TABLE 2: Calculated Rotational Barrier of Amino and Nitro Groups in TATB

method[a]	E(min)[a]	ΔE(amino)[b]	ΔE(nitro)[b]
B3LYP	−1012.114430	42.1	17.9
MP2	−1009.542319	29.3	11.0

[a] Energy of the equilibrium structure in hartrees. [b] Energy difference in kcal/mol.

of internal molecular modes. As listed, the barrier of the amino group is unusually high: 42.1 and 29.3 kcal/mol at the B3LYP and MP2 levels, respectively. The magnitude of this barrier cannot be justified on the basis of hydrogen-bonding interactions alone but rather reinforces our earlier observation of the $C-NH_2$ double-bond character.

The presence of double-bond character in $C-NH_2$ is somewhat anticipated on the basis of classical resonance arguments. The molecular structure of TATB is such that several conjugative interactions are possible. In addition to structure I above, enhanced interaction of the π-donating NH_2 group is positively reinforced with the interaction of the π-accepting NO_2 group, leading to the arrangement depicted in structure II.

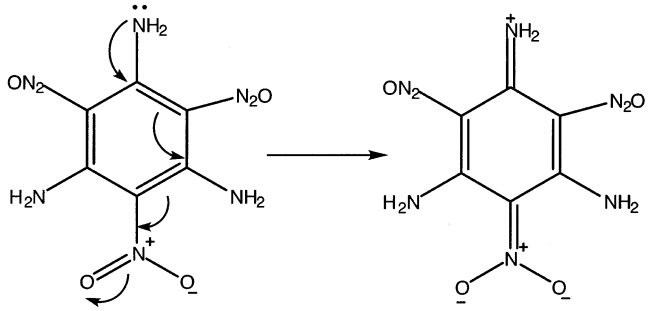

II

In fact, a strong "push−pull" conjugation among the amino and nitro groups around the ring was invoked to explain the exocyclic torsion of the TATB molecular structure.[25] An earlier study on the electron density distribution also supported the presence of radialenelike bonding.[26,27] The fully substituted benzene ring in TATB, however, places a limit on the type of these conjugative interactions, which must be balanced because of saturation and steric effects.

The NO_2 calculated rotational barrier listed in Table 2 is significantly lower than that due to the amino group, 11.0 (17.9) kcal/mol at the MP2 (B3LYP) level. Nevertheless, the magnitude of this barrier is considerably higher than that for comparable molecular systems such as nitroethylene and nitrobenzene: 4.9 and 4.6 kcal/mol, respectively, as calculated at the MP2/6-311G**//MP2/6-31G* level of theory.[12] As we stated previously,[7] the existence of the surrounding bulky amino groups plays an important role in hindering the rotational motion of the nitro group. Upon rotation, the nearest-neighbor oxygen−hydrogen bond, R(O−H), is increased to 2.7 Å from its relatively short length of 1.7−1.8 Å at the equilibrium structure.

It is evident that large discrepancies are manifested between the MP2 and B3LYP results for both rotational barriers. The B3LYP values are 43.7% and 62.7% larger than the MP2 results for the amino and nitro rotational barriers, respectively. The lowering of these barriers at the MP2 level can be attributed to the explicit treatment of electronic correlation that is significant in conjugated systems[12] and to the inclusion of dispersion interactions that are dominant in TATB. It was demonstrated that, in the case of nitroethylene,[12] the MP2-calculated rotational barrier of 4.9 kcal/mol was in excellent agreement with the

TABLE 3: Optimized Molecular Parameters for Amino Rotation[a]

	angles					
	MP2			B3LYP		
parameter	30	60	90	30	60	90
	Bond Lengths					
$R(C_5-C_2)$	1.418	1.411	1.410	1.437	1.433	1.431
$R(C_4-N_{10})$	1.354	1.364	1.366	1.329	1.333	1.335
$R(C_2-N_8)$	1.458	1.461	1.458	1.440	1.448	1.460
$R(N_8-O_{14})$	1.231	1.228	1.228	1.235	1.225	1.218
$R(N_{10}-H_{22})$	1.008	1.008	1.008	1.013	1.011	1.010
$R(O_{18}-H_{24})$	2.483	3.087	3.398	1.864	2.191	2.675
$R(O_{13}-H_{22})$	1.850	1.928	1.952	1.738	1.773	1.794
	Angles					
$C_1-C_4-C_3$	116.8	116.1	115.9	118.2	117.5	116.9
$C_5-C_1-C_4$	122.0	122.7	123.2	120.7	120.8	121.1
$O_{14}-N_8-O_{17}$	123.5	125.0	125.2	120.9	122.6	123.7
$C_3-N_9-O_{18}$	118.2	117.8	117.7	119.0	118.2	118.3
$C_4-N_{10}-H_{19}$	116.7	115.8	115.6	117.5	117.8	117.9
$H_{23}-N_{11}-H_{22}$	121.5	119.5	119.0	124.8	124.2	123.6
$C_6-C_3-N_9$	118.3	118.4	118.1	118.6	118.1	118.3
$C_2-C_6-N_{12}$	121.8	121.4	121.4	121.0	121.1	121.0
	Dihedrals					
$C_3-C_4-C_1-C_5$	5.6	5.1	3.9	6.0	4.7	5.3
$N_8-C_2-C_5-N_{11}$	10.2	13.1	12.9	9.6	11.7	12.3
$O_{16}-N_7-C_1-C_4$	27.4	30.3	33.3	1.0	0.2	1.7
$O_{13}-N_7-C_1-C_5$	21.7	25.9	29.4	1.1	0.3	1.6
$O_{17}-N_8-C_2-C_5$	41.2	55.9	54.8	26.0	36.3	43.7
$O_{14}-N_8-C_2-C_6$	37.1	52.0	49.5	25.1	33.8	41.2
$O_{18}-N_9-C_3-C_6$	48.7	58.5	56.5	26.1	33.6	41.3
$O_{15}-N_9-C_3-C_4$	46.2	57.9	56.3	25.6	36.3	43.8
$H_{22}-N_{10}-C_4-C_1$	3.0	4.7	4.7	2.2	2.9	2.6
$H_{19}-N_{10}-C_4-C_3$	28.5	33.5	34.0	5.6	6.8	9.7
$H_{22}-N_{11}-C_5-C_2$	0.8	0.4	1.0	3.8	6.9	9.7
$H_{20}-N_{11}-C_5-C_1$	25.9	31.5	33.7	4.1	2.8	2.6

[a] Bonds in Å and angles in degrees. Rotation is around the C_6-N_{12} bond in Figure 1.

experimentally determined barrier of 4.83 kcal/mol.[13] A B3LYP calculation on equal computational footing for nitrobenzene provided a barrier of 6.9 kcal/mol, which is 2.3 kcal/mol higher than the MP2 result[12] despite the fact that the intramolecular O−H interaction is much weaker in nitrobenzene, the bond distance being 2.39 Å.

C. Torsional Barriers. To examine the effect of relaxation of internal molecular modes, we calculated the minimum-energy paths connecting the perpendicular transition structures of the amino and nitro groups to the respective equilibrium structures. In the absence of a unique 1D coordinate that describes the rotational motion, we choose the following two dihedral angles as our constrained modes: $\angle X_1NCC_1$ and $\angle X_2NCC_2$, as depicted in III, where X_1 and X_2 are either hydrogen (amino) or oxygen (nitro) atoms.

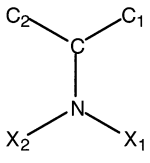

III

We define $\gamma = \angle X_1NCC_1 = \angle X_2NCC_2$ as a fixed parameter and optimize the remainder of the molecular coordinates. This choice allows equal treatment of the angles formed between the planes defined by the ONC and NCC groups of atoms.

Figures 2 and 3 display the fully optimized torsional curves for the amino and nitro groups, respectively, relative to the energy of the respective equilibrium structures. An extended set of optimized molecular parameters for the rotation interval is listed in Tables 3 and 4; these parameters should be of use in the development of a molecular force field for TATB. The lists will also help identify the behavior of the unconstrained molecular parameters in response to this constrained motion.

TABLE 4: Optimized Molecular Parameters for Nitro Rotation[a]

	angles					
	MP2			B3LYP		
parameter	30	60	90	30	60	90
	Bond Lengths					
$R(C_5-C_2)$	1.422	1.402	1.394	1.433	1.407	1.396
$R(C_4-C_{10})$	1.343	1.346	1.344	1.327	1.329	1.330
$R(C_2-C_8)$	1.446	1.457	1.462	1.442	1.465	1.483
$R(N_8-O_{14})$	1.240	1.235	1.238T	1.238	1.228	1.220
$R(O_{14}-H_{21})$	1.830	2.116	2.543	1.798	2.123	2.828
$R(O_{16}-H_{22})$	1.800	1.802	1.757	1.716	1.732	1.738
	Angles					
$C_1-C_4-C_3$	117.8	118.1	118.8	118.9	119.2	119.2
$C_2-N_8-O_{14}$	119.1	117.8	117.3	119.6	118.0	117.4
$C_6-N_{12}-H_{21}$	117.1	116.5	117.2	118.1	119.2	120.4
	Dihedrals					
$C_3-C_4-C_1-C_5$	5.1	4.7	5.8	8.0	4.6	1.9
$N_8-C_2-C_5-N_{11}$	4.8	1.2	1.3	1.7	2.1	2.2
$O_{16}-N_7-C_1-C_4$	28.3	23.2	5.4	1.3	1.1	3.0
$O_{13}-N_7-C_1-C_5$	21.5	18.0	14.8	8.8	5.0	2.2
$O_{18}-N_9-C_3-C_6$	29.5	26.8	14.4	3.0	3.9	2.5
$O_{15}-N_9-C_3-C_4$	22.4	19.1	4.9	1.2	1.2	2.6
$H_{24}-N_{12}-C_6-C_3$	0.3	4.5	9.6	5.0	0.6	5.0
$H_{21}-N_{12}-C_6-C_2$	22.7	29.8	26.1	9.2	16.5	11.4
$H_{22}-N_{10}-C_4-C_1$	0.2	2.2	14.1	1.8	0.5	3.3
$H_{19}-N_{10}-C_4-C_3$	21.5	21.5	13.9	0.9	0.1	3.6
$H_{23}-N_{11}-C_5-C_2$	1.1	28.0	26.2	11.7	16.5	11.6
$H_{20}-N_{11}-C_5-C_1$	22.4	1.8	9.4	4.1	0.4	5.2

[a] Bonds in Å and angles in degrees. Rotation is around the C_2-N_8 bond in Figure 1.

The NH_2 torsional curve has maxima for $\gamma = 90°$ of 25.5 and 17.0 kcal/mol at the B3LYP and MP2 levels, respectively. These values are still larger than typical single-bond torsional barriers. The effect of nuclear relaxation is also significant because these values are reduced by 16.6 (B3LYP) and 12.3 (MP2) kcal/mol from the rigid-body approximation. We note that, at this degree of rotation, the B3LYP method provides a similar result for the rigid-body case: ∼50% higher than the MP2 result. The MP2 energy curve in Figure 2 shows a steep increase for small γ, in contrast to the B3LYP calculations. This is indicative of immediate resistance toward rotation around a bond with significant π character. For $\gamma = 30°$, with rotation around the C_6-N_{12} bond in Figure 1, $\angle H_{24}NC_6C_3$ experiences this full rotation from its corresponding value at the equilibrium structure of 0.2°, in contrast to $\angle H_{21}NC_6C_2$ of 21.5°. Whereas the MP2 barrier at this angle of rotation is 10.1 kcal/mol, representing 68% of the maximum barrier, the B3LYP barrier is only 4.0 kcal/mol at the same degree of rotation. We also note that the only significant changes in the optimized molecular parameters listed in Table 3 from the equilibrium structure are those corresponding to the torsion of neighboring nitro groups and, in the case of MP2, a dramatic increase in the nearest-neighbor O−H bond distance of the rotating amino group, $R(O_{18}H_{24})$. The dihedrals $\angle O_{17}N_8C_2C_5$, $\angle O_{14}N_8C_2C_6$, $\angle O_{18}N_9C_3C_6$, and $\angle O_{15}N_9C_3C_4$ react strongly to the NH_2 rotation, showing a maximum increase of 20° (40°) at the MP2 (B3LYP) levels. These rotations of the nitro group in turn induce smaller rotations of the remainder amino groups: 5−10° for $\angle H_{19}N_{10}C_4C_3$ and $\angle H_{20}N_{11}C_5C_1$.

As for the NO_2 torsional barrier, Figure 3 shows maxima at $\gamma = 90°$ of 10.5 and 5.6 kcal/mol at the B3LYP and MP2 levels, respectively. The full optimization of nuclear coordinates reduces the rigid-body barrier by 70% (B3LYP) and 96% (MP2). Here again, we note that the B3LYP result is 87.5% higher than that obtained by MP2 and that both the B3LYP and MP2 curves in Figure 3 exhibit little change for rotation of up to $\gamma = 30°$. For MP2, this result is expected because the nitro group is already in partial rotation in its equilibrium structure, where $\angle O_{17}NC_2C_5 = 29.1°$ and $\angle O_{14}NC_2C_6 = 22.6°$. This small energy cost of nitro torsions could easily be compensated for when considering the benefit of forming a cyclic network of hydrogen bonds, as is the case in the solid phase.

Interestingly, the MP2-optimized curve is almost identical to a MP2 single-point calculation of the B3LYP-optimized curve reported earlier.[7] Similar to the case for amino rotation, the parameters most affected by the nitro group rotation, as listed in Table 4, are the dihedrals. Most pronounced is the MP2 result for the dihedral $\angle O_{16}N_7C_1C_4$, showing a change from 28 to 5° in the full rotation interval. This effect is also shown in the neighboring amino group with $\angle H_{22}N_{10}C_4C_1$ changing from near zero to 14°. The B3LYP parameters exhibit a much less noticeable variation, with the exception of $\angle H_{21}N_{12}C_6C_2$ that reacts immediately to the nitro rotation with a variation of up to 10°. In addition to the striking differences between MP2 and B3LYP in the energetics of the rotational barrier, the results also provide a further contrasting molecular response upon deformation of these two methods.

Finally, we also considered the fully optimized torsional barrier due to a single-angle rotation, ∠XNCC, where X is an oxygen or hydrogen atom. For $\angle ONCC = 90°$, the barrier is 5.3 (10.5) kcal/mol at the MP2 (B3LYP) levels; both are close to their respective values obtained when a two-angle constraint was imposed. This is not unexpected because adjacent ∠ONCC angles have similar rotations at the equilibrium structure for both methods (Table 1). As for the amino rotation, adjacent ∠HNCC angles differ by as much as 20° at the MP2 level. More importantly, the two-angle constraint affects the pyramidal sp^3 bonding character in this group. For $\angle HNCC = 90°$, we calculated a barrier of 15.0 (15.0) kcal/mol at the MP2 (B3LYP) levels. The MP2-optimized structure yielded a ∠HNH bond angle of 86°, with both hydrogens being out-of-plane as in structure IV below. The B3LYP optimization, however, yielded a structure in which $\angle HNH = 107°$, with the adjacent hydrogen remaining planar with respect to the carbon ring.

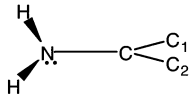

IV

III. Conclusions

We have calculated the amino and nitro group rotational and torsional barriers for TATB at the B3LYP and MP2 levels using the standard 6-311G** basis set. The fully optimized amino and nitro group torsional potential barriers exhibit maxima of 17.0 (25.5) and 5.6 (10.5) kcal/mol at the MP2 (B3LYP) levels, respectively. These values are markedly different from the rigid-body barriers of 29.3 (42.1) for the amino and 11.0 (17.9) kcal/mol for the nitro rotation, respectively, at the MP2 (B3LYP) levels of theory, thus reflecting the importance of full nuclear relaxation. The large barrier associated with the amino rotation is due to the double-bond character of the respective C−N bond, with corresponding conjugative structures that are balanced by steric and saturation effects in this molecule. The MP2 results are 40−85% lower in energy than those determined using B3LYP, clearly demonstrating the need for further assessment and care in choosing an adequate method for the development of a force field for systems that manifest strong intramolecular hydrogen bonding.

Acknowledgment. This work was performed under the auspices of the U.S. Department of Energy at the University of California, Lawrence Livermore National Laboratory, under contract no. W-7405-Eng-48. M.R.M. acknowledges useful discussions with R. Schmidt and P. Pagoria.

References and Notes

(1) Dobratz, B. M. *The Insensitive High Explosive Triaminotrinitrobenzene (TATB): Development and Characterization−1888 to 1994*; Los Alamos National Laboratory: Los Alamos, NM, 1995.
(2) Cady, H. H.; Larson, A. C. *Acta Crystallogr.* **1965**, *18*, 485.
(3) Kolb, J. R.; Rizzo, H. F. *Propellants Explos.* **1979**, *4*, 10.
(4) Son, S. F.; Asay, B. W.; Henson, B. F.; Sander, R. K.; Ali, A. N.; Zielinski, P. M.; Phillips, D. S.; Schwarz, R. B.; Skidmore, C. B. *J. Phys. Chem. B* **1999**, *103*, 5434.
(5) Ledoux, I.; Zyss, J.; Siegel, J. S.; Brienne, J.; Lehn, J. M. *Chem. Phys. Lett.* **1990**, *172*, 440.
(6) Voight-Martin, I. G.; Li, G.; Yakimanski, A.; Chulz, G.; Wolff, J. J. *J. Am. Chem. Soc.* **1996**, *118*, 12830.
(7) Manaa, M. R.; Fried, L. E. *J. Phys. Chem. A.* **2001**, *105*, 6765.
(8) Møller, C.; Plesset, M. S. *Phys. Rev.* **1934**, *46*, 618.
(9) Parr, R. G.; Yang, W. *Density-Functional Theory of Atoms and Molecules;* Oxford Universiy Press: New York, 1989.
(10) Becke, A. D. J. *J. Chem. Phys.* **1993**, *98*, 5648.
(11) Lee, C.; Yang, W.; Parr, R. G. *Phys. Rev. B* **1988**, *37*, 785.
(12) Head-Gordon, M.; Pople, J. A. *Chem. Phys. Lett.* **1990**, *173*, 585.
(13) Meyer, R.; Gammeter, A.; Smith, P.; Kuhne, H.; Nosberger, P.; Gunthard, H. H. *J. Mol. Spectrosc.* **1973**, *46*, 397.
(14) Allen, F. H.; Baalham, C. A.; Lommerse, J. P. M.; Raithby, P. R.; Sparr, E. *Acta Crystallogr., Sect. B* **1997**, *53*, 1017.
(15) Johnson, B. G.; Gill, P. M. W.; Pople, J. A. *J. Chem. Phys.* **1993**, *98*, 5612.
(16) Tsuzuki, S.; Luthi, H. P. *J. Chem. Phys.* **2001**, *114*, 3949.
(17) Perdew, J. P.; Wang, Y. *Phys. Rev. B* **1992**, *45*, 13244.
(18) Zhang, Y.; Pan, W.; Yang, W. *J. Chem. Phys.* **1997**, *107*, 7921.
(19) Wesolowski, T. A.; Parisel, O.; Ellinger, Y.; Weber, J. *J. Phys. Chem. A* **1997**, *101*, 7818.
(20) Rappe, A. K.; Bernstein, E. R. *J. Phys. Chem. A* **2000**, *104*, 6117.
(21) Smith, G. D.; Bharadwaj, R. K. *J. Phys. Chem. B* **1999**, *103*, 3570.
(22) Frisch, M. J.; Trucks, G. W.; Schlegel, H. B.; Scuseria, G. E.; Robb, M. A.; Cheeseman, J. R.; Zakrzewski, V. G.; Montgomery, J. A., Jr.; Stratmann, R. E.; Burant, J. C.; Dapprich, S.; Millam, J. M.; Daniels, A. D.; Kudin, K. N.; Strain, M. C.; Farkas, O.; Tomasi, J.; Barone, V.; Cossi, M.; Cammi, R.; Mennucci, B.; Pomelli, C.; Adamo, C.; Clifford, S.; Ochterski, J.; Petersson, G. A.; Ayala, P. Y.; Cui, Q.; Morokuma, K.; Malick, D. K.; Rabuck, A. D.; Raghavachari, K.; Foresman, J. B.; Cioslowski, J.; Ortiz, J. V.; Stefanov, B. B.; Liu, G.; Liashenko, A.; Piskorz, P.; Komaromi, I.; Gomperts, R.; Martin, R. L.; Fox, D. J.; Keith, T.; Al-Laham, M. A.; Peng, C. Y.; Nanayakkara, A.; Gonzalez, C.; Challacombe, M.; Gill, P. M. W.; Johnson, B. G.; Chen, W.; Wong, M. W.; Andres, J. L.; Head-Gordon, M.; Replogle, E. S.; Pople, J. A. *Gaussian 98*, revision A.4; Gaussian, Inc.: Pittsburgh, PA, 1998.
(23) Heher, W. J.; Radom, L.; Schleyer, P. R.; Pople, J. A. *Ab Initio Molecular Orbital Theory;* Wiley & Sons: New York, 1986.
(24) Wu, C. J.; Fried, L. E. *J. Phys. Chem. A* **2000**, *104*, 6447.
(25) Baldridge, K. K.; Siegel, J. S. *J. Am. Chem. Soc.* **1993**, *115*, 10782.
(26) O'Connell, A. M.; Rae, A. I. M.; Malsen, E. N. *Acta Crystallogr.* **1966**, *21*, 208.
(27) Dawson, B. *Aust. J. Chem.* **1965**, *18*, 595.